JOURNAL OF SOLID STATE CHEMISTRY 1, 159–169 (1970)

A Polymer Model for BeF_2 and SiO_2 Melts†

C. F. BAES, JR.

Reactor Chemistry Division, Oak Ridge National Laboratory, Oak Ridge, Tennessee 37830

Received April 28, 1969

Crystalline BeF_2 and SiO_2 have similar structures in which tetrahedrally coordinated cations (M) are bridged by bi-coordinated anions (Y) producing a network of MY_4 tetrahedra with shared corners. Each compound melts to produce a very viscous liquid which no doubt is highly polymeric. When a basic fluoride is added to BeF_2 or a basic oxide is added to SiO_2, the viscosity of the resulting NY–MY_2 mixtures drops rapidly, presumably because bridging anion linkages have been broken, and the degree of polymerization decreased. This plausible qualitative description has been treated more quantitatively on the assumptions that: (1) The many possible polymeric species M_aY_b which can be formed in such binary mixtures all involve tetrahedrally coordinated M cations and mono- or bi-coordinated Y anions; (2) the stability of each such polymeric species M_aY_b depends primarily on the number of bridging anions (–Y–) and the number of non-bridging anions (–Y) it contains and, to a lesser extent, on the size of rings formed in the cross-linked polymer structures; and finally (3) the activity of species M_aY_b in the melt can be derived from volume fractions according to Flory's approximation for the entropy of mixing and from a heat-of-mixing term. Although the evaluation of component activities (a_{MY_2} and a_{NY}) from this model requires extensive numerical calculations, the model is inherently a simple one with but three adjustable parameters. It fits observed activities quite well over the full composition range in the LiF–BeF_2 system and in several silicate systems for which accurate data are available.

As crystalline solids, SiO_2 and BeF_2 have three-dimensional network structures made up of SiO_4^{4-} and BeF_4^{2-} tetrahedra which share corners. Thus the anions O^{2-} and F^- all are bridged between two of the tetrahedrally coordinated central cations Si^{4+} and Be^{2+}. Each compound readily forms glasses in which there seems little doubt that the tetrahedral coordination of the cation and the two-fold coordination of the anion is largely retained (*1*). Just above the melting points the liquids are very viscous, suggesting that they are still highly polymeric.

The binary molten mixtures which are formed when basic oxides are added to SiO_2 or basic fluorides are added to BeF_2 are characterized by a rapidly falling viscosity (*2*) as the amount of the basic component is increased. This is presumably because bridging anion linkages are broken.

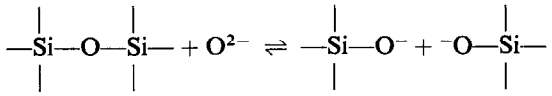

† This research was sponsored by the U.S. Atomic Energy Commission under contract with the Union Carbide Corporation.

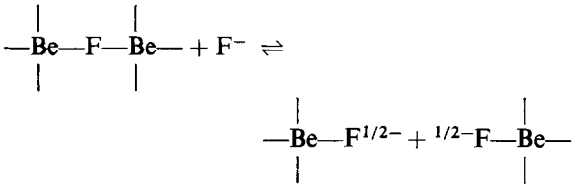

(1)

Førland (*3*) has interpreted the SiO_2 and BeF_2 liquidus data in such binary mixtures in terms of random mixing of bridging and non-bridging anions. Masson (*4*, *5*) has considered the other end of the composition range in silica systems. According to his model, as SiO_2 is added to a basic oxide (NO) the monomeric anion SiO_4^{4-} is formed and later, as a deficiency of O^{2-} develops with increasing silica content, oxide ions are shared to produce increasingly long polymer anions.

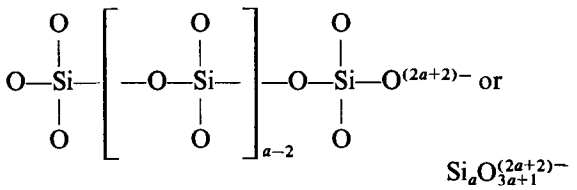

$Si_aO_{3a+1}^{(2a+2)-}$

In the limit, the chains become infinitely long and the silicon-to-oxygen ratio reaches 1:3, which corresponds to 50 m/o silica in an $NO–SiO_2$ system.

More recently Pretnar (*6*) has proposed a model for such melts in which again a single sequence of increasingly polymeric species is proposed but with the interesting difference that condensed or cross-linked structures are included. Thus while the initial species are the same as those of Masson, the one following $Si_5O_{16}^{12-}$ is a ring $Si_6O_{18}^{12-}$ rather than a chain $Si_6O_{19}^{14-}$. In subsequent more polymeric species, side-chains of SiO_3^{2-} units are grown until another six-membered ring can be formed. With extended polymerization, Pretnar envisions the growth of spherically shaped crystalline aggregates which have the cristobalite structure. This single sequence of structures (analogous to boundary II in Fig. 1) permits the entire composition range to be included in the model. While Masson assumed an equilibrium condition among the polymer chains wherein the activity of each species was proportional to its mole fraction, Pretner assumes an equilibrium condition between bridging oxide (–O–), non-bridging oxide ($–O^{1-}$) and free oxide ions (O^{2-}) analogous to reaction (1) above in which the activity of each kind of oxide is proportional to its fraction of the total oxide.

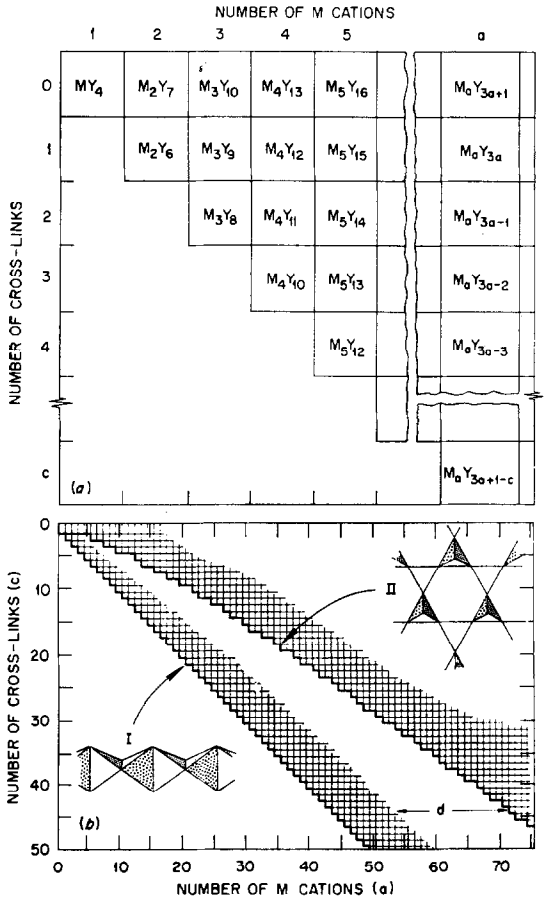

FIG. 1. The array of possible polymeric anionic species M_aY_b. (a) The initial species formed; (b) The two boundaries which result if the most highly cross-linked species are formed (I) by sharing edges of MY_4 tetrahedra to produce chains (M_aY_{2a+2}) or (II) by sharing corners of tetrahedra to produce network polymers with six-numbered rings as in crystalline SiO_2 or BeF_2.

The present model was inspired by Masson's approach and was developed (*7*) while the author was still unaware of Pretnar's treatment. It contains some features of both previous models in that while all the linear polymers of Masson are included, so are all the condensed structures of Pretnar, as well as all possible combinations of both. An equilibrium condition analogous to that of Masson is assumed, but with the activities of species expressed in volume fractions rather than mole fractions. Heat of mixing effects are also included. Although the calculation of component activities from this model requires extended summations by means of a high speed computer, the model at its present stage of development has the virtue that it is a simple one with a small number of adjustable parameters. It will be compared with recent data on activities in the $LiF–BeF_2$ system as well as with other data which are available for SiO_2 systems. The notation to be used is summarized in Table I.

1. Formulation of the Model

1.1 *Polymeric Anion Complexes.* In this model we will consider all the possible structures M_aY_b (omitting charge) in which the cation M (Be^{2+} or Si^{4+}) has a coordination number of 4 and the anion Y (F^- or O^{2-}) either is shared between two cations or is coordinated to only one. All these complexes have a negative charge since, except for infinitely large ones, the ratio b/a is always greater than 2.

All such structures which are possible can be classified by the array in Fig. 1. In each row, the number (a) of central cations increases from left to right; in each column the number (c) of cross links increases from top to bottom. Thus the first row, which begins with the monomer MY_4 and extends to indefinitely large values of a by the successive addition of MY_3 groups, includes all the structures of Masson (M_aY_{3a+1}). These may be linear or branched chain polymers. In the second row one cross link has been formed, i.e., one ring has been closed. This lowers by one the number (b) of Y

TABLE I

NOTATION

a, b	The number of cations M and anions Y in a polynuclear anionic species M_aY_b.
c	The number of cross links or rings in the species M_aY_b, equal to $3a + 1 - b$.
s, t	The number of shared (–Y–) and unshared (–Y) anions in M_aY_b: $s = 4a - b$; $t = 2b - 4a$.
d	The deficiency (if any) in the number of M cations in M_aY_b needed to produce a specified number of six-numbered rings (Figs. 1, 2 and Eq. (9)).
$K_{a,b}$	Equilibrium constant for Reaction 10.
$\alpha = G/RT$	Free energy parameter associated with polymerization (Eqs. (10) and (11)).
$\beta = H/RT$	Heat of mixing parameter (Eq. (18)).
$\gamma = G_r/RT$	Free energy parameter associated with instability of rings containing less than six M cations.
$n_{a,b}, \Phi_{a,b}, \mathscr{A}_{a,b}$	The number of moles, the volume fraction (Eq. (15)), and the activity of species M_aY_b (Eqs. (20) and (21)). Subscript 0, 1 denotes free Y.
n_1, n_2, X_1, X_2	The number of moles and the mole fractions of components NY(1) and MY_2(2).
$\mathscr{A}_1, \mathscr{A}_2, f_1, f_2$	The activity and the activity coefficient ($=\mathscr{A}/X$) of components NY and MY_2.

anions present for a given number (a) of M cations and, hence, the general formula here is M_aY_{3a}. Continuing to more highly cross-linked structures, the general formula is M_aY_{3a+1-c}, where c is the number of cross links.

Thus it may be seen that if the formula of a complex is specified—if a and b are specified—the number of cross links c is also determined.

$$c = 3a + 1 - b \tag{2}$$

Furthermore, the total number of M–Y links in a given complex is $4a$, and this number must equal twice the number of shared anions (s) plus the number of unshared anions (t)

$$2s + t = 4a. \tag{3}$$

Also

$$s + t = b. \tag{4}$$

Solving for the number of shared (s) and unshared anions (t)

$$s = 4a - b; \quad t = 2b - 4a, \tag{5}$$

we see that s and t, like c, are uniquely specified by the indices a and b,

It is important to note that while the formula of a complex thus specifies the number of cross links and the number of shared and unshared anions present, it of course does not specify the detailed structure of the complex; i.e., in this classification the numerous structural isomers of a given formula M_aY_b with various branchings and ring sizes are not distinguished.

While in Fig. 1, a and c may become indefinitely large, an important variable of the model is the location of the boundary at the left of the array which defines the most highly cross-linked structures which are formed; i.e., those complexes which contain the minimum allowable value of a for a given value of c. Two limiting cases will be considered, one in which a minimum ring size of two MY_4 tetrahedra is assumed and one in which a minimum ring size of six is assumed:

(I) A minimum ring size of two corresponds to the formation of chains in the most highly cross-linked structures, chains in which tetrahedral edges are shared

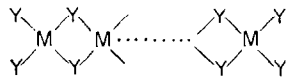

, M_aY_{2a+2} (6)

In this case $a(\min) = c + 1$.

(II) If the minimum ring size is assumed to be six, the most highly cross-linked structures which are then possible are fragments of one of the crystalline forms of silica or BeF_2. Here the minimum possible values of a for an increasing number of cross-links or rings in a structure were determined by considering an ever larger portion of the tridymite lattice in the form of a right hexagonal prism (Fig. 2). The ratio of width to height was chosen to give the maximum ratio of shared to unshared Y anions. The relationship of a to b for such a crystallite is†

$$b = 2a + (9a/4)^{2/3}. \tag{7}$$

The expression for c is

$$c = a + 1 - (9a/4)^{2/3}. \tag{8}$$

While these equations have exact integer solutions for b and c only for the regular hexagonal crystallites from which they were derived Eq. (8) was used to locate the boundary of the array for other crystal

† This expression is almost identical to that obtained by Pretnar (Ref. 6) for spherical crystalline fragments of cristobalite.

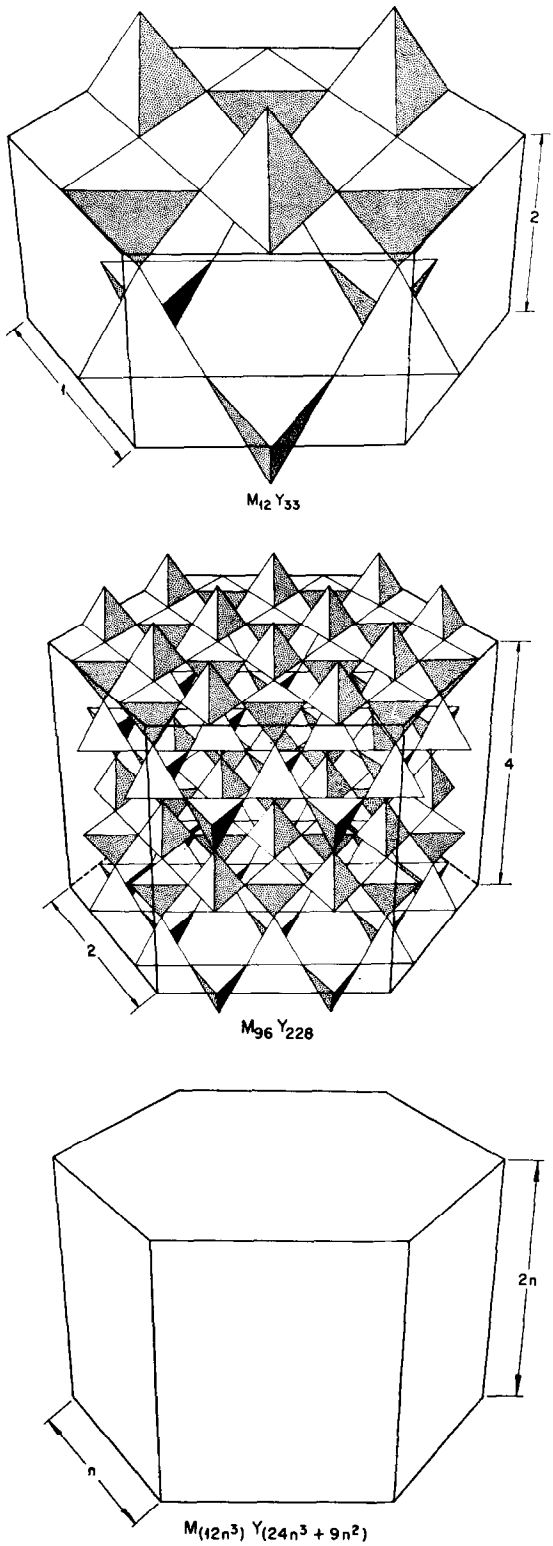

FIG. 2.

fragments of intermediate size by the approximate procedure of rounding off the non-integer values of c obtained for each integer value of a to the next lower integer. The resulting estimates thus obtained for the minimum values of a for each value of c were found to agree within ± 1 with other estimates obtained by inspection of fragments of the tridymite and cristobalite lattice in which the number of M atoms was increased from 1 to 50.

As the polymer size of the most condensed structure is increased, in both cases a b/a ratio of 2 is approached corresponding to the pure liquid end member MY_2, however, the limiting structures produced in the two cases are completely different. In the first case, the limiting structures are infinite chains of tetrahedra with shared edges, analogous to the structure of $BeCl_2$ (*8*). In the second, the limiting structures are three dimensional networks analogous to the SiO_2 structures. In both cases as one moves away from the most condensed structures (i.e., to the right in the array in Fig. 1) the rings may of course increase in size, or side chains may appear in the various structural isomers, or both. Nevertheless, the choice of one or the other of these structures as the most highly cross-linked species which can form has a strong influence on the predicted degree of polymerization as the MY_2 content of the solution is increased. This in turn, as we shall see, influences the predicted behavior of the activity coefficients of the components. Therefore, it will be desirable to vary the contributions of these two limiting structures. This will be done by assuming that all complexes shown in the array in Fig. 1 can be formed, but that those to the left of boundary II suffer an increasing loss in stability, because of the necessary replacement of shared tetrahedral corners by shared tetrahedral edges—linkages which are presumably more strained and less stable as the distance to the left of boundary II is increased. This distance will be designated by the integer d

$$d = a(\text{min, II}) - a. \tag{9}$$

1.2 *Stability of Complexes.* In the following generalized polymerization reaction

$$a\,MY_4 \rightleftharpoons M_aY_b + (4a - b)\,Y, \tag{10}$$

on proceeding from left to right we find the following

FIG. 2. Crystal fragments of the tridymite structure in which there are a minimum number of unshared tetrahedral corners (Y) for a given number of tetrahedra (MY_4). The vertical dimension in each case denotes the number of hexagonal layers of MY_4 tetrahedral; the other dimension refers to the number of tetrahedra along an edge of each layer.

changes in the numbers of shared, unshared, and free anions Y (Eqs. (5))

$$(\text{-Y-});\ 0 \rightarrow 4a - b,$$
$$(\text{-Y});\ 4a \rightarrow 2b - 4a,$$
$$(\text{Y});\ 0 \rightarrow 4a - b,$$

The net result is that $8a - 2b$ unshared Y ions disappear and $4a - b$ each of shared and free Y anions are formed. Thus this reaction may be viewed as the reverse of reaction (1) taken $4a - b$ times. The accompanying free energy change will be approximated as

$$\Delta G_{a,b} = -(4a - b)\, G + (d)\, G_r, \qquad (11)$$

where G represents the free energy change associated with reaction (1). The term $(d)G_r$ denotes the loss of stability which will be assigned to complexes which lie to the left of boundary II in Fig. 1; d is an integer which specifies the distance left of the boundary (for all complexes to the right of the boundary $d = 0$) and G, is a free energy parameter. The equilibrium constant for reaction (10) may be approximated

$$K_{a,b} = \frac{\mathscr{A}_{a,b}\mathscr{A}_{0,1}^{4a-b}}{\mathscr{A}_{1,4}^{a}} = \exp[(4a - b)\alpha - (d)\gamma], \qquad (12)$$

wherein $\alpha = G/RT$ and $\gamma = G_r/RT$. The standard states to which $\Delta G_{a,b}$ and the various activities $\mathscr{A}_{a,b}$ refer are, with one exception, hypothetical liquids

$$NY, N_2[MY_4], \quad \text{and} \quad N_{(b-2a)}[M_aY_b],$$

in which N is the only cation and the anions have in each case a single formula—a single set of a and b values—but include all possible structural isomers in equilibrium amounts. The activity of such a hypothetical component in a mixture is expressed

$$\mathscr{A}(N_{b-2a}M_aY_b) = (\mathscr{A}_N^{b-2a})(\mathscr{A}_{a,b}) \cong \mathscr{A}_{a,b}, \qquad (13)$$

wherein the activity of cation N is taken as unity. Since N is the only kind of cation, it seems reasonable to assume that there will be only small entropy and heat effects associated with its self-mixing when the hypothetical pure liquids are mixed.

For species to the right of the boundary II in Fig. 1 the above approximation for the value of $K_{a,b}$ would be exact if the free energy of each hypothetical pure liquid could be expressed as the sum of contributions which are proportional to the number of each kind of atom present; i.e., if

$$G^0(N_{b-2a}M_aY_b) = (b - 2a)\, G_N + (a)\, G_M + (4a - b)\, G_{Y(s)} + (2b - 4a)\, G_{Y(t)},$$

wherein G_N, G_M, $G_{Y(s)}$, and $G_{Y(t)}$ denote the free energy contribution per gram atom of N, M, shared Y, and unshared Y atoms, respectively. Such a relationship might well be expected to approximate H^0. Furthermore, since the hypothetical liquids which serve as standard states contain all the structural isomers of the complex anion M_aY_b, there is no contribution to S^0 from isomerization and hence an expression of this form might also approximate S^0. Consequently equations 11 and 12 seem reasonable approximations.

1.3 *Activity of Complexes.* In order to make use of the above expression (12) for the equilibrium constant $K_{a,b}$, it is first necessary to relate the activities of Y, MY_4 and M_aY_b to the concentrations of the various species in mixtures. To obtain these relationships it will first be assumed that, as in mixtures of linear polymers (*9*), the entropy of mixing can be represented in terms of volume fractions

$$\Delta S_m = R\sum n_i \ln \Phi_i, \qquad (14)$$

or

$$\Delta S_m = Rn_{0,1} \ln \Phi_{0,1} + R \sum_c \sum_a n_{a,b} \ln \Phi_{a,b},$$

(again, c is the number of cross links and is equal to $3a + 1 - b$. Here and elsewhere, the limits of the double summations are $c = 0$ to ∞ and $a = c + 1$ to ∞. The subscripts 0,1; 1,4; and a,b denote, respectively, the anions Y, MY_4, and M_aY_b.) Since the volume of each complex should be determined almost entirely by the number of anions it contains, we will approximate the volume fractions by

$$\Phi_{0,1} = \frac{n_{0,1}}{n_1 + 2n_2}; \quad \Phi_{1,4} = \frac{4n_{1,4}}{n_1 + 2n_2};$$
$$\Phi_{a,b} = \frac{bn_{a,b}}{n_1 + 2n_2} \qquad (15)$$

where n_1 and n_2 denote moles of NY and MY_2 respectively. The following material balance relationships then may be written:

$$\Phi_{0,1} + \sum\sum \Phi_{a,b} = 1, \qquad (16)$$

$$\sum\sum (a/b)\Phi_{a,b} = \frac{n_2}{n_1 + 2n_2} = \frac{X_2}{1 + X_2}, \qquad (17)$$

where it may be noted that the first term in each double summation (with $c = 0$ and $a = 1$) corresponds to the monomer MY_4; X_2 is the stoichiometric mole fraction of MY_2 in the mixture.

The heat of mixing will be approximated by

$$\Delta H_m = H\Phi_{0,1} \sum\sum (2b - 4a) n_{a,b}, \qquad (18)$$

in which the summation term represents the number of moles of unshared Y's in the mixture. The product

of this times the fraction of Y anions which are free ($\Phi_{0,1}$) should be proportional to the moles of free Y – unshared Y "contacts" in the mixture. These contacts are assumed to produce the principal contribution to the heat of mixing.

The expressions for the entropy of mixing (Eq. (14)) and the heat of mixing (Eq. (18)) may be introduced into

$$RT\ln\mathscr{A}_{a,b}=\frac{\partial(\Delta H_m - T\Delta S_m)}{\partial n_{a.b}} \qquad (19)$$

to give the following expressions for the activity of Y and M_aY_b

$$\mathscr{A}_{0,1}=\Phi_{0,1}\exp\left\{(1-\Phi_{0,1})\left[1-\frac{1}{\bar{b}}\right]+4\beta(1-\Phi_{0,1})\left[\frac{1-\Phi_{0,1}}{2}-\frac{X_2}{1+X_2}\right]\right\}, \qquad (20)$$

$$\mathscr{A}_{a,b}=\Phi_{a,b}\exp\left\{1-b+b(1-\Phi_{0,1})\left[1-\frac{1}{\bar{b}}\right]+4\beta\Phi_{0,1}\left[\frac{b\Phi_{0,1}}{2}-a+\frac{bX_2}{1+X_2}\right]\right\}, \qquad (21)$$

wherein $\beta = H/RT$ and $\bar{b}$ is the average number of Y anions per polymeric species; i.e., a polymerization number

$$\bar{b}=\frac{\sum\sum bn_{a,b}}{\sum\sum n_{a,b}}=\frac{\sum\sum \Phi_{a,b}}{\sum\sum (1/b)\Phi_{a,b}}. \qquad (22)$$

1.4 *Distribution of Complexes.* Introducing these expressions for activities into the equilibrium constant expression (Eq. (12)), we obtain the following equation for the volume fraction of a species M_aY_b

$$\Phi_{a,b}=(UV)^a V^{c-1}/\exp(1+d\gamma), \qquad (23)$$

wherein

$$U=e\Phi_{1,4},$$

$$V=(1/\Phi_{0,1})\exp\left\{\alpha+4\beta\left[\Phi_{0,1}-\tfrac{1}{2}+\frac{X_2}{1+X_2}\right]-1\right\}.$$

The volume fraction of M_aY_b in a given mixture thus is determined largely by two factors, one raised to the power a and the other to the power $c-1$. As a consequence, the concentration in a given mixture of successive species with increasing a or with increasing c falls logarithmically. As the composition is changed however, the concentration of a given species rises to a maximum and then falls (Fig. 3).

1.5 *Activity of Components.* The activity of NY is taken to be equal to that of free Y—since $\mathscr{A}_N$ is assumed to be unity (Eq. (13))—and so is given by Eq. (20). The activity of MY_2 ($\mathscr{A}_2$) should be

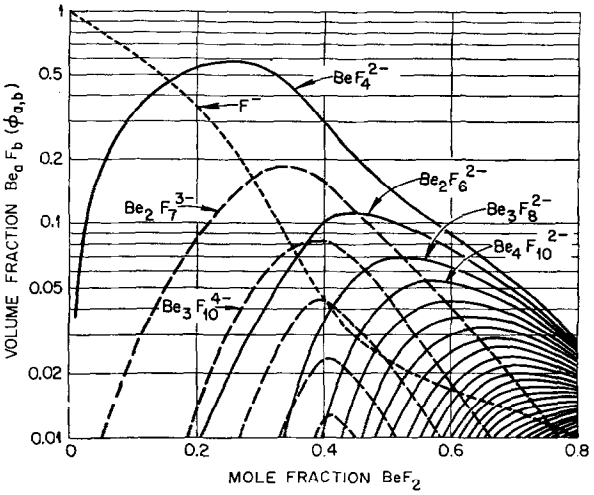

FIG. 3. Volume fraction of some polymeric species in LiF–BeF_2 melts at ~650°C. Species (Be_aF_{3a+1}) from the top row of the array in Fig. 1 are represented by dashed lines. Species (Be_aF_{2a+2}) along boundary I of Fig. 1 are denoted by full lines.

proportional to the quotient $\mathscr{A}_{1,4}/\mathscr{A}_{0,1}^2$. Upon introducing the appropriate expressions from Eqs. (20) and (21), and choosing a proportionality constant such that $\mathscr{A}_2$ becomes unity as X_2 approaches unity, we obtain

$$\mathscr{A}_2=(\Phi_{1,4}/\Phi_{0,1}^2)\exp\left\{2\alpha+4\beta(1+\Phi_{0,1})\times\left[\Phi_{0,1}+\frac{2X_2}{1+X_2}\right]-4\beta+2(1-\Phi_{0,1})\times\left[1-\frac{1}{\bar{b}}\right]-3\right\} \qquad (24)$$

[The proportionality constant was determined from the following limiting values:

$X_2=1$; $a_2=1$; $\Phi_{0,1}=0$; $\bar{b}=\infty$; and $\Phi_{1,4}/\Phi_{0,1}^2=\exp(1-2\alpha)$. The limiting value of $\Phi_{1,4}/\Phi_{0,1}^2$ as X_2 approaches unity was deduced as follows: if, in Eq. 23, γ is taken to be 0, then

$$\sum\sum\Phi_{a,b}=\frac{1}{e}\sum_{c=0}^{\infty}V^{c-1}\sum_{a=c+1}^{\infty}(UV)^a$$

$$=\frac{U}{e(1-UV)}\sum_{c=0}^{\infty}(UV^2)^c$$

$$=U/[e(1-UV)(1-UV^2)]$$

Here first $\sum_0^\infty (UV)^n$ is replaced by $1/(1-UV)$ and then $\sum_0^\infty (UV^2)$ is replaced by $1/(1-UV^2)$. The products UV and UV^2 each must fall in the range 0–1 if $\sum\sum \Phi_{a,b}$ is to be <1. In the limit $UV^2 \to [\exp(2\alpha-1)]\Phi_{1,4}/\Phi_{0,1}^2 \to 1$. Hence $\Phi_{1,4}/\Phi_{0,1}^2 \to \exp(1-2\alpha)$. With $\gamma \neq 0$, analogous arguments show that UV^2 and $\Phi_{1,4}/\Phi_1^2$ still approach the same limits as $\Gamma X_2 \to 1$.]

1.6 *Calculation Procedure.* With given values of the parameters α, β, and γ, a melt composition (X_2) is chosen and trial values of $\Phi_{0,1}$ and $\Phi_{1,4}$ are selected. The summations

$$\sum\sum \Phi_{a,b} \quad \text{and} \quad \sum\sum (a/b)\,\Phi_{a,b}$$

are then evaluated using Eq. (23) and tested in the material balance Eqs. (16) and (17). $\Phi_{0,1}$ and $\Phi_{1,4}$ are refined by iteration until they satisfy these boundary conditions.

[This iteration procedure is simplified considerably if $\gamma = 0$ since then $\sum\sum \Phi_{a,b}$ may be replaced by the rational expression

$$U/[e(1-UV)(1-UV^2)]$$

(see above) and $\Phi_{1,4}$ is given explicitly by

$$\Phi_{1,4} = Z - \sqrt{Z^2 - 1/(e^2 V^3)}$$

wherein

$$Z = \frac{e(1-\Phi_{0,1})V(1+V)+1}{2e^2(1-\Phi_{0,1})V^3}$$

Hence only $\Phi_{0,1}$ need be refined and with but one summation determined numerically.]

Once $\Phi_{0,1}$ and $\Phi_{1,4}$ values have been determined for a chosen melt composition the average value of b is determined from the summation $\sum\sum (1/b)\Phi_{a,b}$ (Eq. 22) and finally $\mathscr{A}_1$ and $\mathscr{A}_2$ are calculated by means of Eqs. (20) and (24).

The summations converge more slowly as X_2 increases, especially as γ is made larger. The iterations required to determine $\Phi_{0,1}$ and $\Phi_{1,4}$ become more lengthy and also more hazardous in the sense that too large a change in $\Phi_{0,1}$ or $\Phi_{1,4}$ can easily cause a summation to diverge. Using the CDC-1604 computer and carrying summations to $c = 3000$, calculations could be carried to $X_2 \sim 0.95$ with $\gamma = 0$, to $X_2 \sim 0.60$ with $\gamma = 0.2$, and to $X_2 \sim 0.40$ with $\gamma = 0.5$. The limit in X_2 beyond which convergence in the summations could not be attained below $c = 3000$ arises because as γ is increased, crystalline aggregates are favored over chains and since the former contain a greater ratio of unshared to shared Y anions for a given size of polymer, it is necessary that much larger polymers be formed as X_2 is increased and the number of Y anions available for M cations is decreased.

2. Results

Before comparing this model with observed activities of the components in NY–MY_2 systems, let us examine the effect of each of the adjustable parameters on the predicted behavior of the activity coefficients f_1 (of NY) and f_2 (of MY_2). The calculated curves in Fig. 4 show that the free energy parameter α has perhaps the most profound influence upon behavior. As α is decreased (Fig. 4a), corresponding to a decreasing tendency toward polymerization, both f_1 and f_2 show more negative deviations from ideality. When the parameter β is decreased (Fig. 4b), corresponding to a more exothermic heat

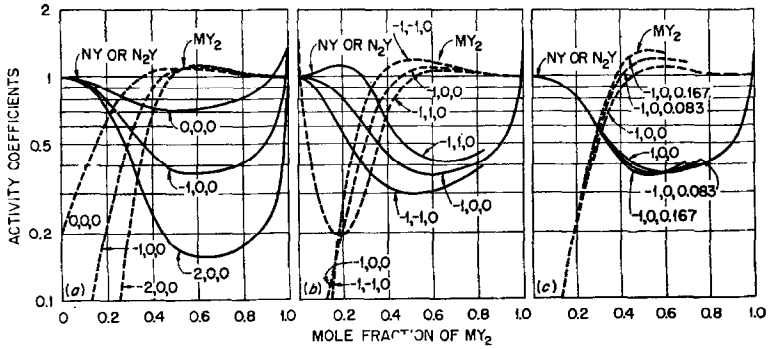

FIG. 4. Effect of variation of adjustable parameters on calculated activity coefficients in the system NY–MY_2 or N_2Y–MY_2. Numbers given for each curve denote the values of α, β, and γ, respectively: (a) Variation of α; (b) Variation of β; (c) Variation of γ.

of interaction between bound and unbound Y anions, f_1 is uniformly lowered while f_2 is decreased below $X_2 \sim 0.17$ and is increased above this value. As the parameter γ is increased above zero (Fig. 4c), corresponding to an increased instability of rings smaller than 6-numbered ones in the polymeric species, the principal effect is to increase f_2 at higher values of X_2 reflecting the more rapid approach of $\mathscr{A}_2$ to unity as larger polymers are formed. The limiting value of f_2 as X_2 approaches zero is

$$(f_2)_{X_2 \to 0} = 4\exp(2\alpha + 4\beta - 3)$$

The corresponding limit for f_1 is

$$(f_1)_{X_1 \to 0} = e/2$$

at least when $\gamma = 0$.

2.1 *LiF–BeF_2 System.* Smoothed values of the activity coefficients of BeF_2 from the recent EMF measurements of Hitch and Baes (*10*) in this system are compared with curves calculated from the present model in Fig. 5. The parameters α and γ were assumed to vary linearly with $1/T$, $°K^{-1}$

$$\alpha = \alpha^0 + \alpha'/T; \qquad \gamma = \gamma^0 + \gamma'/T$$

and all five parameters—α^0, α', γ^0, γ', and β—were adjusted by a nonlinear least squares computer program (*11*) to give the best fit to the EMF data (Table II). Included in the fit were points taken from the LiF liquidus curve (*12*) which yield f_{LiF} values in the high LiF composition range.

The overall fit to the EMF data was within 2σ, σ being based on the observed scatter in the EMF data which was typically ± 1 to ± 3 mV. This agreement is considered quite satisfactory in view of the essential simplicity of the model and the small number of parameters which it employs.

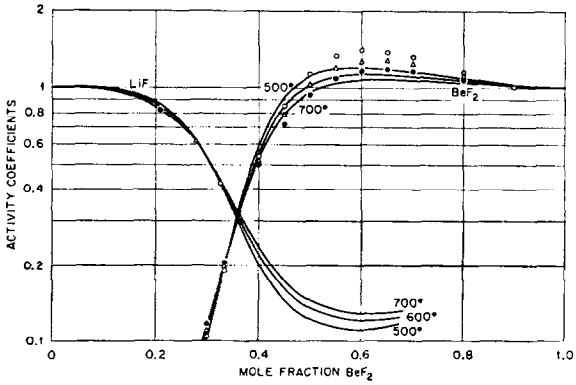

FIG. 5. The LiF–BeF_2 system. Points on the BeF_2 curves are from smoothed EMF data (Ref. *10*); points on the LiF curves are from the liquidus data (Ref. *12*); curves were calculated using parameters in Table II.

Distribution curves for some of the species $Be_aF_b^{(b-2a)-}$ calculated from the adjusted parameters at 645° are shown in Fig. 3. These serve to indicate that such polymeric systems are highly polydisperse and ought not to be described in terms of just a few species.

2.2 *FeO–SiO_2.* Silicate systems are difficult to study because of the high temperatures involved and hence accurate activity measurements are relatively few. Not surprisingly, considering its importance in steel making, the FeO–SiO_2 system is the silicate system for which perhaps the most accurate such data are available. The measurements of FeO activity by Bodsworth (*13*) agree well with those of Schulmann and Ensio (*14*), both showing that f_{FeO} has a very low dependence on temperature. Their data are compared with a curve calculated from the present model (Fig. 6) with a least squares adjustment of α and β. One point representing f_{SiO_2} at the silica (tridymite saturated) liquidus (*15*), calculated from a recent value for the heat of fusion of SiO_2 (2.5 kcal/mole) reported by Kleppa (*16*), was used to aid in adjusting the value of γ. Because of the high value of γ (Table II), calculations were not carried beyond $X_{SiO_2} = 0.36$. (Since the FeO–SiO_2 mixtures involved contained some Fe(III), the data were corrected by the procedure described by Masson (*4*)

$$\mathscr{A}_{FeO} = \mathscr{A}_{FeO}(\text{obs})(N^0_{Fe++}/N_{Fe++})$$

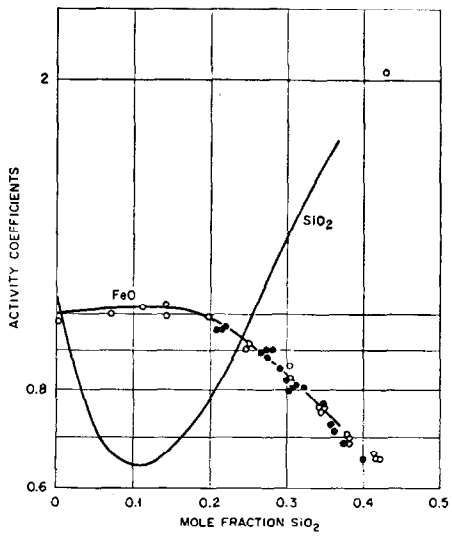

FIG. 6. FeO–SiO_2 system. Open circles (Ref. *13*) and closed circles (Ref. *14*) on FeO curves are at various temperatures in the range 1259–1407°C. The point on the SiO_2 curve is at the liquidus composition at 1300°C (Refs. *15*, *16*). The curves were calculated using parameters in Table II.

TABLE II

PARAMETER VALUES FOR SEVERAL SYSTEMS

System	Temperature (°C)	α	β	γ	r_+ (Å)	Z_+^2/r_+
$FeO-SiO_2$	1300	−0.09	0.47	0.64	0.75	5.33
$MnO-SiO_2$	1600	−1.27	0.72	0.33	0.80	5.00
$PbO-SiO_2$	1000	−1.66	0.22	0.11	1.21	3.31
$LiF-BeF_2$	500	−2.39	0.49	0.07		
	600	−2.32	0.43	0.02	0.60	1.67
	700	−2.25	0.39	−0.02		

wherein the observed activities of FeO were multiplied by the Fe^{++} cation fraction (N^0_{Fe++}) in the pure "FeO" standard state (*17*) to which the observed activities were referred originally and were divided by the Fe^{++} cation fraction (N_{Fe++}) found in the mixtures.)

The fit of the calculated curve for the activity coefficient of FeO (Fig. 6) is excellent, being within the small scatter of the data. The curve for SiO_2 generated by the model, however, is less reliable since it has a strong dependence on the choice of γ, which in turn is based on the single point for γ_{SiO_2} at the SiO_2 liquidus.

2.3 *The PbO–SiO_2 System.* Recent EMF data of Sridhar and Jeffes (*18*) in this system agree well with earlier equilibrium measurements of Richardson *et al.* (*19*) (Fig. 7). The curves calculated by the present model were adjusted to the EMF results. Again, points from the tridymite liquidus (*20*) were used to aid in adjusting γ and thus better establish the SiO_2 curve. The fit is somewhat less satisfactory than the previous ones, but probably does not greatly exceed the uncertainty of the data.

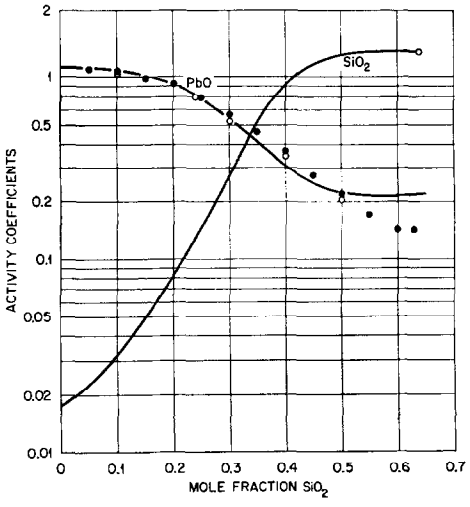

FIG. 7. The PbO–SiO_2 system. Open circles (Ref. *18*) and closed circles (Ref. *19*) on the PbO curve and the point on the SiO_2 liquidus (Refs. *16*, *20*) all are at 1000°C. The curves were calculated using the parameters in Table II.

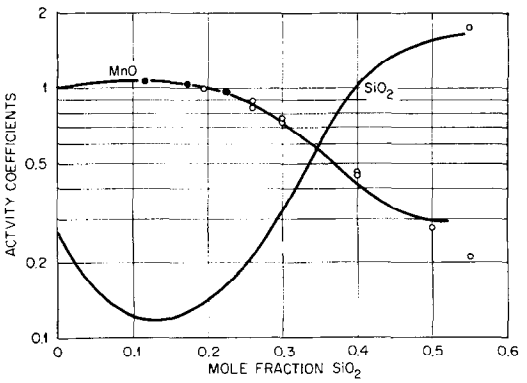

FIG. 8. The MnO–SiO_2 system. Open circles on MnO curve are based on smoothed data at 1500 and 1650°C (Ref. *21*); closed circles are from MnO liquidus (Refs. *22*, *4*) and open circle on SiO_2 curve is from the SiO_2 liquidus at 1600°C (Refs. *22*, *16*). The curves are calculated using parameters in Table II.

2.4 *The MnO–SiO_2 System.* The smoothed data of Abraham *et al.* (*21*) for $\mathscr{A}_{MnO}$, referred to the solid as standard state were adjusted to the supercooled-liquid standard state using the liquidus curve of Glasser (*22*) and a heat of fusion estimated by Masson (*4*). The fit of the model to the data again is satisfactory (Fig. 8).

Discussion and Conclusions

The present model is an improvement over the ones proposed previously by Masson (*4*, *5*) and Pretnar (*6*) in that it includes all the polymeric

species of 4-coordinate Si^{4+} ro Be^{2+} which might be expected to form in silicate or fluoroberyllate melts. In addition, use of the volume fraction to express the entropy of mixing of the hypothetical components seems a better approximation than does Masson's use of the mole fraction in view of the great range in the size of the species being mixed. Finally, it is reasonable to suppose that a heat effect would accompany this hypothetical mixing process because of the interaction of unshared anions (–Y) of the polymeric species M_aY_b with the (next-nearest neighbor) free anions (Y). Although the present model is much more cumbersome mathematically than are either of the previous ones, it remains an essentially simple one with a small number of parameters and is consistent with the limited amount of accurate data thus far available for component activities in binary SiO_2 and BeF_2 systems.

Perhaps the most important assumption of the present model, and of the previous ones, is that the cation M is always coordinated tetrahedrally by Y. It is this condition, of course, which requires that extensive polymerization take place as the mole fraction of MY_2 in a mixture is increased and the ratio of Y to M falls significantly below 4. Yet it might well be observed that, after all, the electrostatic energy of a planar MY_3 group is only slightly less than that of a tetrahedral MY_4 group of the same M–Y distance, and hence we might reasonably expect a decrease in the coordination number of M to accompany—and diminish—growing polymerization. While such a provision perhaps ought to be tested in a refinement of the present model (though this would by no means be simple) it seems quite reasonable to accept the present assumption as an adequate approximation in view of the almost universal occurrence of tetrahedral SiO_4 groups in crystalline silicates and the occurrence of similar BeF_4 groups in BeF_2 and crystalline fluoroberyllates.

Upon accepting the basic assumption that M remains fully 4-coordinated, we are driven to the conclusion that chain structures involving shared tetrahedral edges (i.e., double bridges of Y anions) are important in melts of high MY_2 content in systems such as LiF–BeF_2 and PbO–SiO_2 which do not exhibit prior separation of pure or nearly pure MY_2. Otherwise, the network structures which form must become so very large in order to share enough of the limited supply of Y anions in such melts that not only are they scarcely credible, but also they must lead to separation of an MY_2 rich phase. For example if a melt with an MY_2 mole fraction of 0.7 contains only network polymers such as those pictured in Fig. 2, the *average* number of M cations per polymer ion must be at least 63, whereas if chain polymers M_aY_{2a+2} are assumed, the average degree of polymerization which is necessary falls to less than 5.

The usefulness of the present model in predicting the thermodynamic properties of other silicate or fluoroberyllate melts will depend to a large extent on success in relating the adjustable parameters α, β, and γ (or G, H, and G_r) to the properties of the pure components, in particular the basic component NY (or N_2Y). The few systems for which parameter values have been determined thus far (Table II) permit us only a few qualitative observations about such possible correlations. The heat of mixing parameter β (or H) while positive in every case, shows no consistent trend with ion size. (This parameter, it should be recalled, refers to the hypothetical mixing of the polymer species; it is not related in any simple way to the usual heat of mixing of NY and MY_2.) Both parameters α and β do, however, show a consistent trend with increasing cation size (Fe^{++} to Pb^{++}) in the case of silicates and, in terms of Z^2/r_+, these trends include the LiF–BeF_2 system. Thus, as might be expected, α becomes more negative and the depolymerization reaction (Eq. 1) is shifted to the right as the counter ion N becomes larger or more basic and, hence, provides less competition with M for the anion Y. At the same time γ decreases, corresponding to an increasing stability of chain polymers and a lesser tendency toward separation of a pure MY_2 phase.

References

1. B. E. Warren and C. F. Hill, *Z. Krist.* **89**, 481 (1934).
2. S. Cantor, W. T. Ward, and C. T. Moynihan, *J. Chem. Phys.* **50**, 2874 (1969).
3. T. Forland, *in* "Fused Salts" (B. R. Sundheim, Ed.), p. 156, McGraw Hill, New York (1964).
4. C. R. Masson, *Proc. Roy. Soc. (London)*, **A287**, 201 (1965).
5. C. R. Masson, *J. Am. Ceram. Soc.* **51**, No. 3, 134 (1968).
6. B. Pretnar, *Ber. der Bunsengeselshaft furPhysikal. Chem.* **72**, No. 7, 773 (1968).
7. C. F. Baes, Jr., Oak Ridge National Laboratory Rept., ORNL-4076, March, 1967, p. 15.
8. R. E. Rundle and P. H. Lewis, *J. Chem. Phys.* **20**, 132 (1952).
9. P. J. Flory, "Principles of Polymer Chemistry," pp. 495–540, Cornell University Press, Ithaca, New York (1953).
10. B. F. Hitch and C. F. Baes, Jr., *Inorg. Chem.*, **9**, 201, (1969).
11. W. R. Busing and H. A. Levy, "ORGLS, A General Fortran Least Squares Program," Oak Ridge National Laboratory Rept., ORNL-TM-271, August 7, 1962.
12. R. E. Thoma, H. Insley, H. A. Friedman, and G. M. Hebert, *J. Nucl. Mat.*, **27**, No. 2, 166 (1968).

13. C. BODSWORTH, *J. Iron and Steel Inst.*, **193**, 13 (1959).
14. R. SCHULMANN AND P. J. ENSIO, *J. Metals*, **3**, 401 (1951).
15. N. L. BOWEN AND J. F. SCHAIRER, *Am. J. Sci.*, 5th Ser., **24**, 200 (1932).
16. J. L. HOLM AND O. J. KLEPPA, *Geochem. et Cosmochem. Acta*, **31**, 2289 (1967).
17. L. S. DARKEN AND R. W. GURRY, *J. Am. Chem. Soc.*, **67**, 1398 (1945); *loc. cit.*, **69**, 798 (1946).
18. R. SRIDHAR AND J. H. E. JEFFES, *Trans. Inst. Mining Met.*, **76**, c44 (1967).
19. F. D. RICHARDSON AND L. E. WEBB, *Bulletin of the Institute of Mining and Metallurgy*, **584**, 529 (1955).
20. R. F. CELLER, A. S. CREAMER, AND E. N. BUNTING, *J. Res., Natl. Bur. Std.*, **13**, 237 (1934).
21. K. P. ABRAHAM, M. W. DAVIES, AND F. D. RICHARDSON, *J. Iron Steel Inst.*, **196**, 82 (1960).
22. F. P. GLASSER, *Am. J. of Sci.*, **256**, 398 (1958).